

(RESEARCH ARTICLE)



## Evaluation of axial velocity and wall pressure models for nozzle bench mark using computational fluid dynamics

Okechukwu T Onah <sup>1,\*</sup>, Ifeanyi A Nnaji <sup>1</sup> and Azubuike M Nwankwo <sup>2</sup>

<sup>1</sup> Mechanical and Production Engineering, Enugu State University of Science and Technology, Enugu, Nigeria.

<sup>2</sup> Mechanical Engineering, Caritas University Amorji-Nike, Enugu Nigeria.

GSC Advanced Engineering and Technology, 2022, 04(01), 012–024

Publication history: Received on 07 May 2022; revised on 14 June 2022; accepted on 16 June 2022

Article DOI: <https://doi.org/10.30574/gsaet.2022.4.1.0041>

### Abstract

Computational Fluid Dynamics (CFD) was used for the analysis of food and drug administration (FDA) benchmark study for biomedical flow transition. An idealized medical device is presented within this thesis and the CFD predictions of pressure and velocity are compared against experimental measurements of pressure and velocity. Fluid flow transition considered were  $Re=500$ ,  $Re=2000$ , and  $Re=6500$  and four simulation models of laminar, k-omega, k-omega SST and k-epsilon based on inlet throat  $Re_{th}=500$ , 2000 and 6500. K-omega SST used for mesh independence determination for 0.0008, 0.0004 and 0.0002 element sizes showed good matched velocity 5.9m/sec with 0.0004 and 0.0002. Axial velocity at centerline for  $Re_{th}=500$ , 2000 and 6500 at line  $X=0$ , showed maximum difference of 77.4% for velocity at centerline 0.08m and 19% for wall pressure at -0.09m suddenly expansion at laminar region Reynolds number 500. Besides, 65.6% and 17.2% were obtained at  $Re=2000$ , which agrees with the CFD simulations and experimental measurements. Nevertheless,  $Re=6500$  models were in good agreement at 49.6% velocity centerline and 8.10% pressure drop, except in laminar region. Also, downstream of simulation of  $Re_{th}=6500$ , other models disappeared which demonstrated K-epsilon model best at Reynolds number turbulent region. Categorically, wall pressure showed negligible axial pressure gradient at centerline with drop in normalization argument of experimental data from 0 to -120N/m<sup>2</sup> counterbalanced at  $Re_{th}=500$ . This deduction could be drawn by disparity of pressure transducer in entire experiment data run.

**Keywords:** Nozzle Bench Mark; Axial Velocity; Computational Fluid Dynamics (Cfd); Wall Pressures; Models

### 1. Introduction

In biomedical applications, CFD is used in designing and analyzing medical device, it can help with visualization of a particular problem, and provide insight into patterns within a flow field. However, the practice of using CFD simulations in assessing viability of medical devices is not well established. As such U.S. Food & Drug Administration (FDA) have designed a computational inter laboratory study (with 28 independent groups) to validate CFD techniques and produce experimental parameters to support CFD verification and validation [1]. The thesis therefore focuses on evaluating CFD performance of Nozzle Benchmark of 2D axisymmetric model using Simulation models for prediction blood fluid flow transition for FDA which is one out of numerous techniques of solving numerical problems of Navier-Stokes equations (NSE), in the fluid dynamics areas have found it need in biomedical area [2], [3]; [4]; and [5]. This technique represents and handle complex anatomical geometries with ease and also enable simulations on massively parallel computing architectures [3]. Works of [5], [6], [3] have been applied in LBM for complex transitional flows of anatomical geometries and found efficient and effective. However, effort has not been made to appraise its effectiveness in FDA nozzle benchmark area. It is overbearing, to discover suitability of benchmark using methods without application [7]. LBM application to FDA nozzle benchmark was only for laminar cases. Previous works done on computation transition

\* Corresponding author: Okechukwu T Onah

Mechanical and Production Engineering, Enugu State University of Science and Technology, Enugu, Nigeria.

flow using LBM by [5] and [3] was for moderate Reynolds number. Therefore, there is need to evaluate simple LBM scheme, without employing complex collision synthetic models at turbulence inflow, to accurately predict benchmarked FDA result, focuses on transition flow regime of Reynolds number between 2000 and 6500 only. Comparative analysis was for *Velocities*, shear stresses, pressures and jet breakdown location with simulations.

U.S. Food & Drug Administration created an initiative to establish CFD simulation as a regulatory tool for medical scheme. Two 'benchmark' flow models with specific parameters were tested for providing accurate experimental datasets in the [8] publication. Experimental results are a useful basis for validating accuracy of CFD simulation and assessing its capacity in development and improvement of medical device. This disquisition focuses on nozzle benchmark model and compares experimental measurement of pressure and velocity provided by Particle image velocimetry (PIV) testing and compares it against CFD results. The ideal medical device made up of four sections: inlet tube, gradual-change section, tube throat and outlet tube. Inlet tube and outlet tube have diameter of 0.012m, throat has a diameter of 0.004m. The cone-shaped "gradual-change" section connects the inlet with throat and has a length of 0.22685m, nozzle has a length of 0.04m. The flow will enter through inlet and then experience a gradual convergence and go through the narrow nozzle throat before it increases at expansion region and flows through the outlet tube. The outlet length is 30 times size of the diameter, 0.36m, which gives enough space for fluid flow full development. The inlet length is calculated using Equation 1.

$$L_e = 4.4D Re^{\frac{1}{6}} \quad (1)$$

The numerical methodology employed were based on laminar, ([www.thermal-engineering.org/what-is-reynolds](http://www.thermal-engineering.org/what-is-reynolds)), where flow rate and tube throat Reynolds number is 500, near transition and turbulent tube throat Reynolds number is 2000 and 6500, used for determination of free stream velocities that allowed calculating first layer height  $Y^+$  ([www.cfd-online.com](http://www.cfd-online.com)),

CFD, a valuable tool for characterizing flow fields by predicting velocity, pressure, and shear stress using numerical techniques. Over 50 years, CFD application have extended from observing any kind flow around airfoil and automobile to improvement and assessment of blood-contacting devices [9] and [10]. The advantages of CFD in designing medical device includes that it provides insight in performance without costly prototypes, providing data assessment at critical regions and predicting difficult measuring quantities which influence blood damage [11] and [12]. Although U.S. Food & Drug Administration have no CFD simulation need in evaluating blood contacting medical device, but heart valves international standard does [13] and [14]. [15] Recognizes Implantable circulatory support device experimental validation with CFD simulation for flow fields characterization in and around these devices, and assess potentials of hemolytic and thrombogenic. However, [15] and [13] standards indicate that CFD usage be limited to design stage which is more appropriate for evaluating relative changes than assessing absolute quantities in design [15]. CFD regulatory tool does not predict value of blood damage. Hence the focus on transitional flow regime of Reynolds number 2000 and 6500. Physical quantities of velocities, shear stresses, pressures and jet breakdown location are compared with simulations. Furthermore, insight into questions like when, where, whether, and how Re transition flow is provided.

## 2. Material and methods

The materials are: geometry of nozzle benchmark models, computer, ANSYS fluent simulation, flow conditions at inlet for laminar flow ( $Re=500$ ), transitional flow ( $Re =2000$ ), and flow of turbulent ( $Re=6500$ ). The various turbulence models used to resolve fluid flow were 7 in total: the  $k-\omega$  model,  $k-\omega$  SST model, Spalart Allmaras model, Transition SST model, laminar model,  $k-\epsilon$  model and Reynolds Stress model.  $k-\epsilon$  and Reynolds Stress model has a  $y^+$  value of 30 and turbulence models has  $y^+$  value as was given in equation (1)

**Table 1** Nozzle Model Flow Conditions

Flow rate (m <sup>3</sup> /s)	Inlet Re	Throat Re	Inlet velocity $u_0$	Freestream velocity
$5.21 \times 10^6$	167	500	0.0461 ms <sup>-1</sup>	0.4143 m/s
$2.08 \times 10^5$	667	2000	0.1842 ms <sup>-1</sup>	1.6572 m/s
$6.77 \times 10^5$	2167	6500	0.5985 ms <sup>-1</sup>	5.3859 m/s

The equation used to calculate velocities is Reynolds Equation shown as Equation 3 from equation 2 below, and wall distance is calculated using Equations 3 to 5 and is displayed in Tables 1 and 2.

$$L_e = 4.4D Re^{\frac{1}{6}} \quad (2)$$

$$Re = \frac{\rho U_{freestream} L_{boundary\ layer}}{\mu} \quad (3)$$

$$C_f = (2\log_{10}(Re_x) - 0.65)^{-2.3} \text{ for } Re_x < 10^9 \quad (4)$$

$$\tau_w = C_f \cdot \frac{1}{2} \rho U_{freestream}^2 \quad (3.4)$$

$$U_* = \sqrt{\frac{\tau_w}{\rho}} \quad (4) \quad y = \frac{y^+ \mu}{\rho u_*} \quad (5)$$

**Table 2** Wall distance according to flow conditions

	Re =500	Re=2000	Re=6500
Wall distance (m) (when y+ =1)	6.8×10 <sup>-5</sup> m	2.2×10 <sup>-5</sup> m	8.1×10 <sup>-6</sup> m
Wall distance (m) (when y+=30)	2.0×10 <sup>-3</sup> m	6.6 × 10 <sup>-4</sup> m	2.4 × 10 <sup>-4</sup> m

Description of Nozzle Benchmark Model Design of A 2D-axisymmetric axial nozzle model geometry inlet length of 0.23m and outlet length of 0.36m and tube throat of 0.04m, Figure 1, created in solid work and imported in the Ansys work bench 2020R1, with incompressible fluid blood.

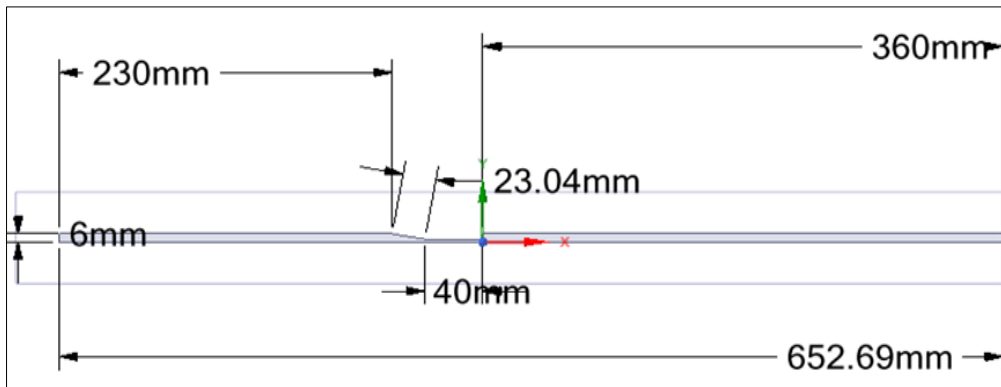


**Figure 1** Geometry of 2D axisymmetric axial nozzle model

Then CFD FLUENT SOLVER edge sizing of Figures 1 and 2 default growth rate used to generate meshes Figures 3, Figure 4 and Figure 5 for each of 0.0008m, 0.0004m and 0.0002m element sizes.

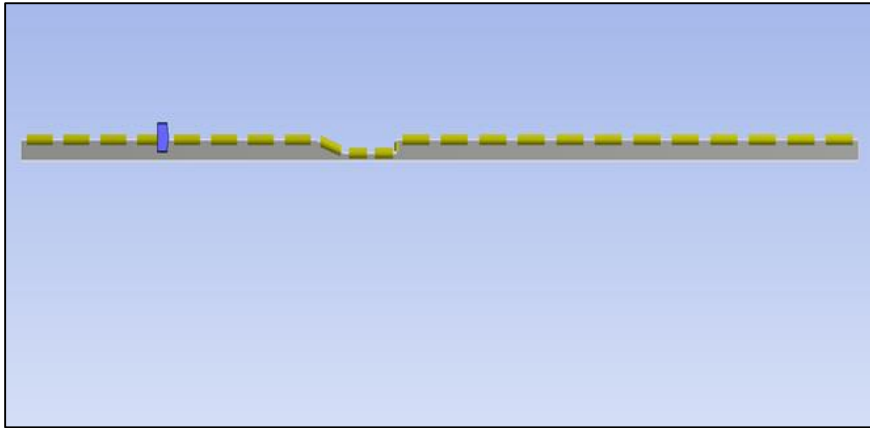


**Figure 2** Edge Sizing

**Table 3** Details of 'Edge Sizing – Sizing

<b>Scope</b>	
<b>Scope Method</b>	<b>Geometry Selection</b>
Geometry	5 Edges
<b>Definition</b>	
Suppressed	No
Type	Element Size
Element Size	Default (3.2636e-002 m)
<b>Advanced</b>	
Behavior	Soft
Growth Rate	Default (1.2)
Capture Curvature	No
Capture Proximity	No
Bias Type	No Bias

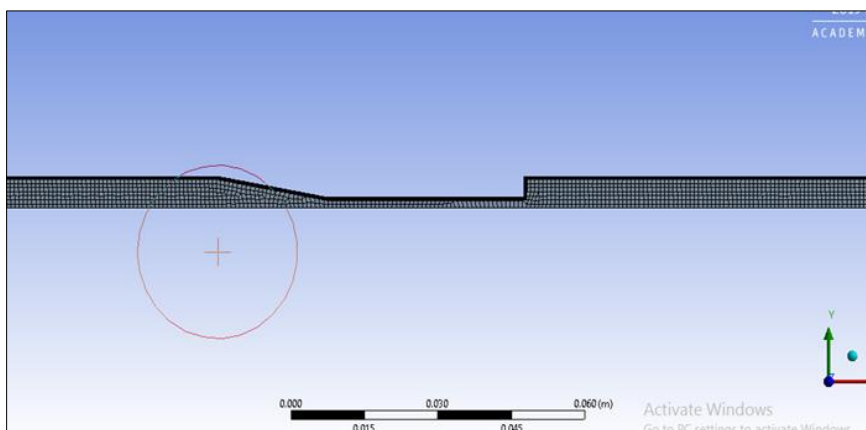


**Figure 3** Mesh of element size 0.0008

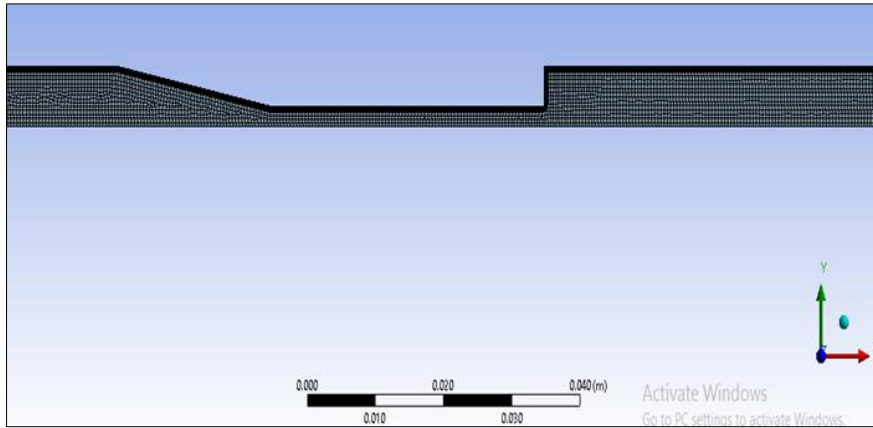


**Figure 4** Mesh of element size 0.0004

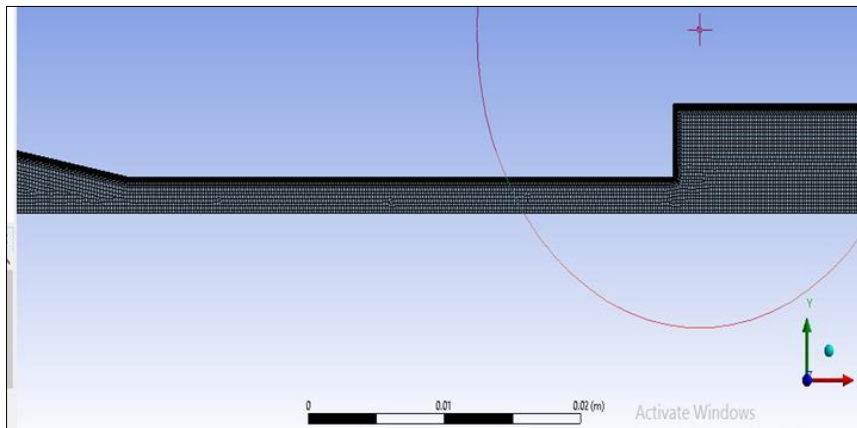


**Figure 5** Mesh of element size 0.0002

The next which is set-up used for initialization and running calculation for 10000 iterations Figures 6, Figure 7 and Figure 8. Numerical solution accuracy presented is contingent on the accurateness of mesh structure and boundary condition specified. Mesh convergence is an important part of ensuring that a solution is valid. By monitoring the residual RMS error and ensuring that variables (pressure drop) do not significantly change with the refinement of mesh. Table 4 shows information about mesh sizes used when trying to solve flow problem.

**Table 4** Mesh Information

Element Size (m)	Nodes	Elements	Pressure Drop (Pa)
0.0008	13421	12647	21907
0.0004	34610	33169	21512
0.0002	112291	109651	21111

The  $K-\omega$  SST model arbitrarily chosen for mesh independence study and Reynolds number 6500 was chosen with inlet velocity  $0.5985 \text{ ms}^{-1}$ . The convergence criteria was set at  $1 \times 10^{-3}$  and a convergence tolerance of  $10^{-7}$  was reached during the hybrid initialization. The residuals were given 1000 iterations for convergence and although most of plots converge around the  $10^{-7}$  and shows good agreement the continuity plot plateaus at around  $1.1 \times 10^{-3}$  for all meshes. Figures 6, Figure 7 and Figure 8, thus illustrate the scaled residuals plot at different element sizes. 0.0008 takes 200 iterations to reach a steady-state whereas the other meshes reach a steady-state somewhere around the 150<sup>th</sup> iteration, an indication of higher degree of accuracy.

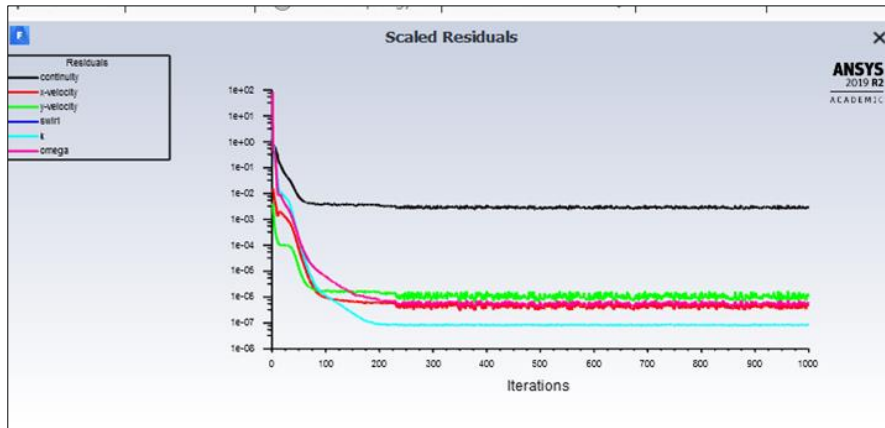


Figure 6 Simulation iteration of Scaled residual value for 0.0008 mesh

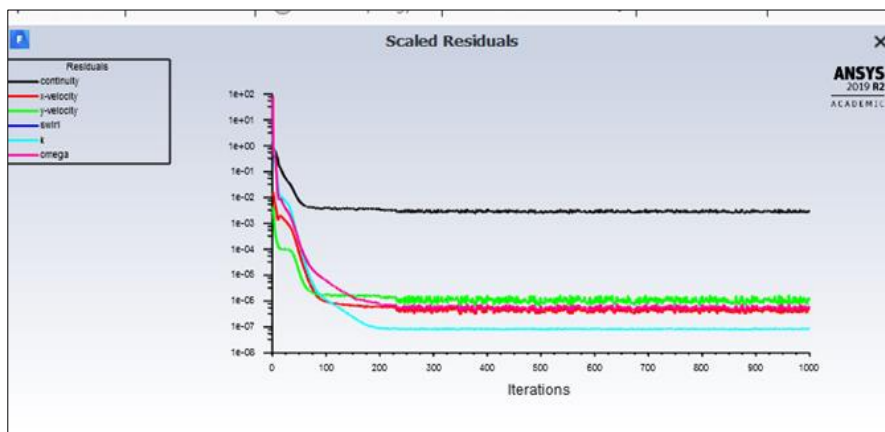


Figure 7 Simulation iteration of Scaled residual value for 0.0004 mesh

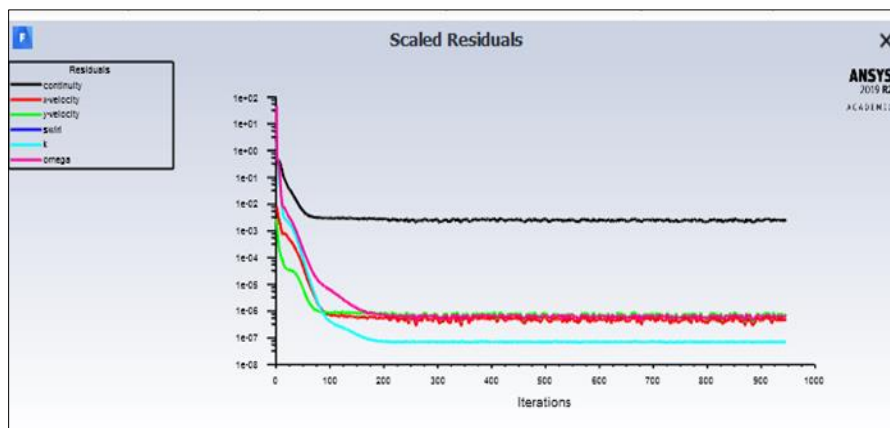


Figure 8 Simulation iteration of Scaled residual value for 0.0002 me

### 3. Results and discussion

Velocity and pressure contours of each element sizes is shown in Figures 9 - 14 respectively. Velocity component of element size 0.0008 slowed down at 5.6m//sec is different from velocities at same point of 0.0004 and 0.0002 element sizes However, velocities at 0.0004 and 0.0002 element sizes started at 6.6m/s and 6.59m/s with 0.01% difference and agreed at velocity 5.9m/sec. Based on inference, 0.0004 element size was now chosen as mesh independence for subsequent analysis and simulation for determination of axial velocity at centreline, wall Pressure and axial velocity at

different points using K-epsilon, Laminar, K-omega and K-omega-SST models. These effects on models were studied at before and after sudden expansion exchange of 0.02m.

Table 5 show different flow rates, throat and inlet Reynolds number. Table 6 showed Reynolds number and calculated inlet velocities while Table 7 shows no of elements, nodes, and element sizes and pressure drops.

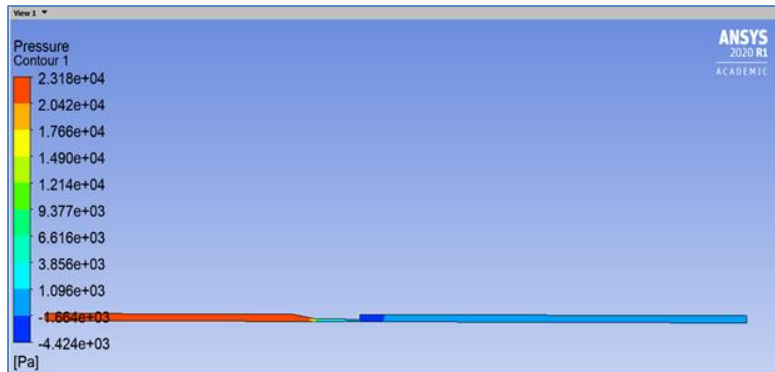


**Figure 9** Pressures Contour of 0.0008 element size

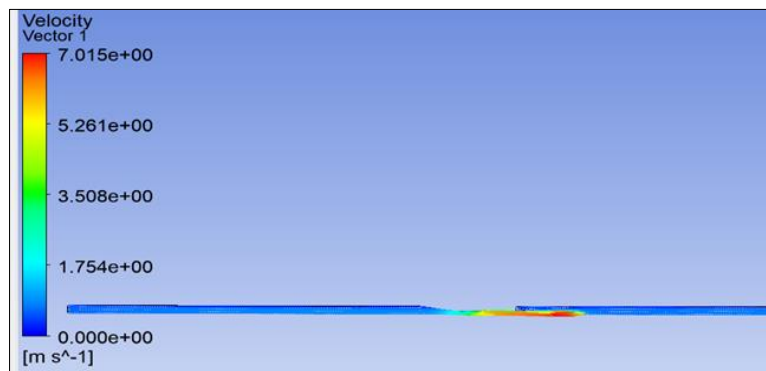


**Figure 10** Velocity Contours of 0.0008 element size

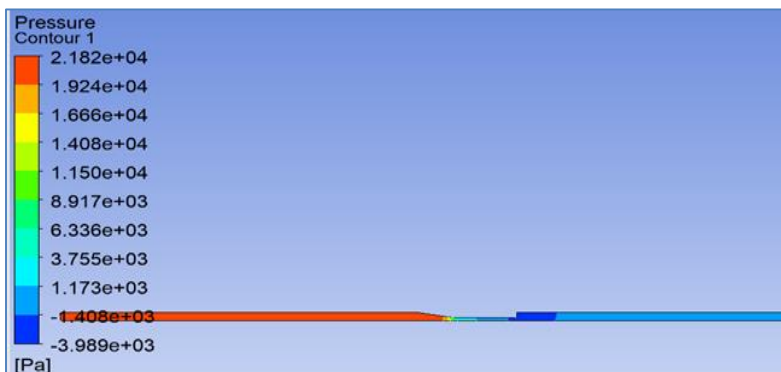


**Figure 11** Pressure Contours of 0.0004 element

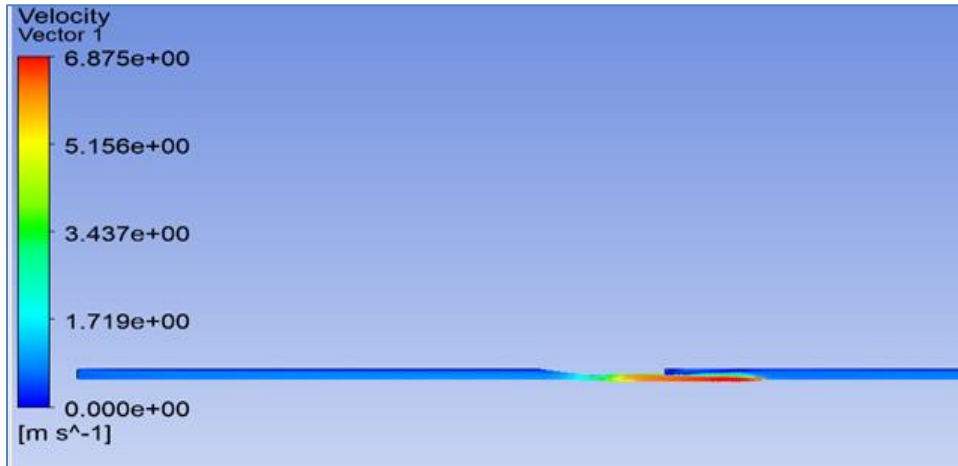


Figure 12 Velocity Contours of 0.0004 element size

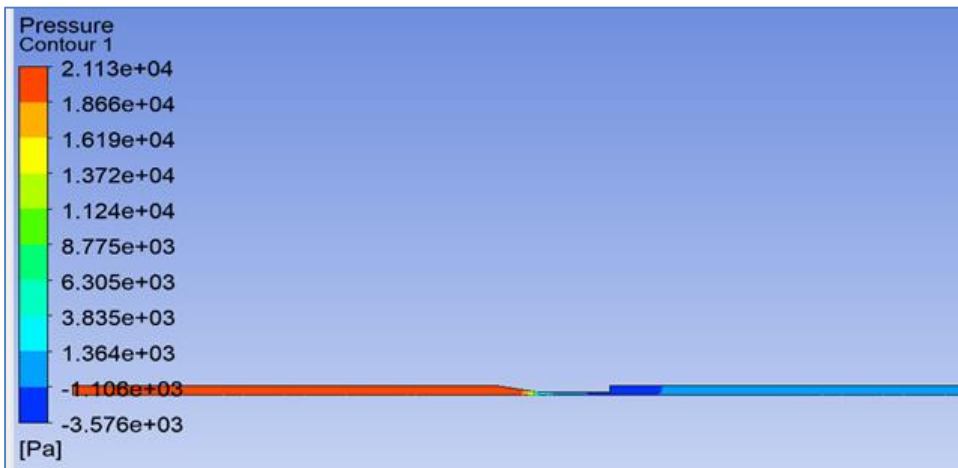


Figure 13 Pressure contours of 0.0002 element size

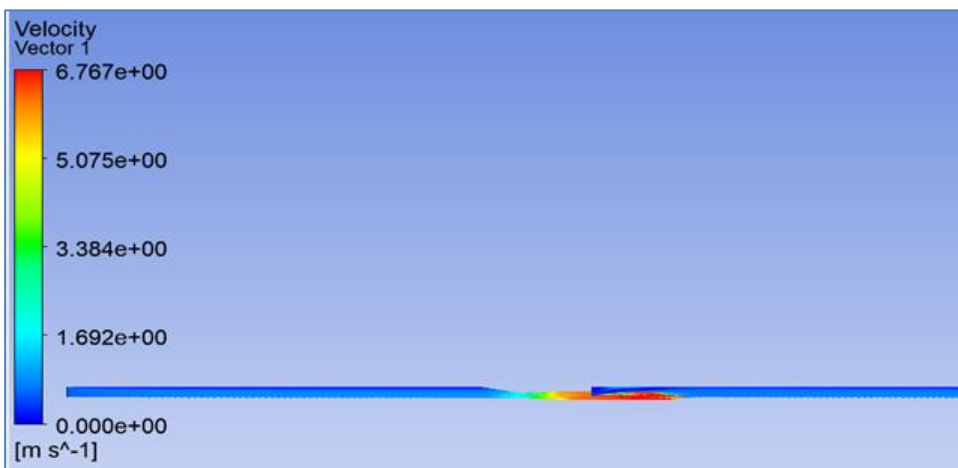
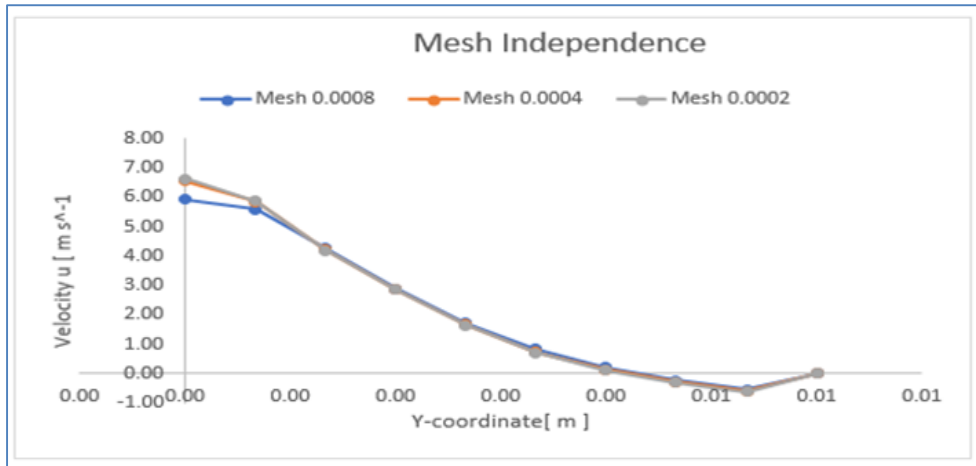


Figure 14 Velocity contours of 0.0002 element size





**Figure 15** Mesh independence determination

**Table 5** Different flow rate tube throat and tube inlet Reynolds number

Flow Rate (m <sup>3</sup> /s)	Tube Throat Reynolds Number	Tube Inlet Reynolds Number
5.21 x 10 <sup>6</sup>	500	167
2.08 x 10 <sup>5</sup>	2000	667
6.77 x 10 <sup>5</sup>	6500	2167

**Table 6** Reynolds number and inlet velocities

Re	Inlet Velocity (m/s)
6500	0.5985
2000	0.1842
500	0.04613

**Table 7** Number of elements, nodes, element sizes and pressure drops

Elements NO	Nodes	Element Size	Pressure Drop(pa)
16401	17181	0.0008	23132.2
39862	41274	0.0004	21747.4
118394	120986	0.0002	21006.8

Comparative study of axial velocity models at centreline for Tube throat Reynolds number  $Re_{th}$  for  $a = 500$ ,  $b = 2000$  and  $c = 6500$  at line  $X=0$ , experimental data presented in Figure 16.

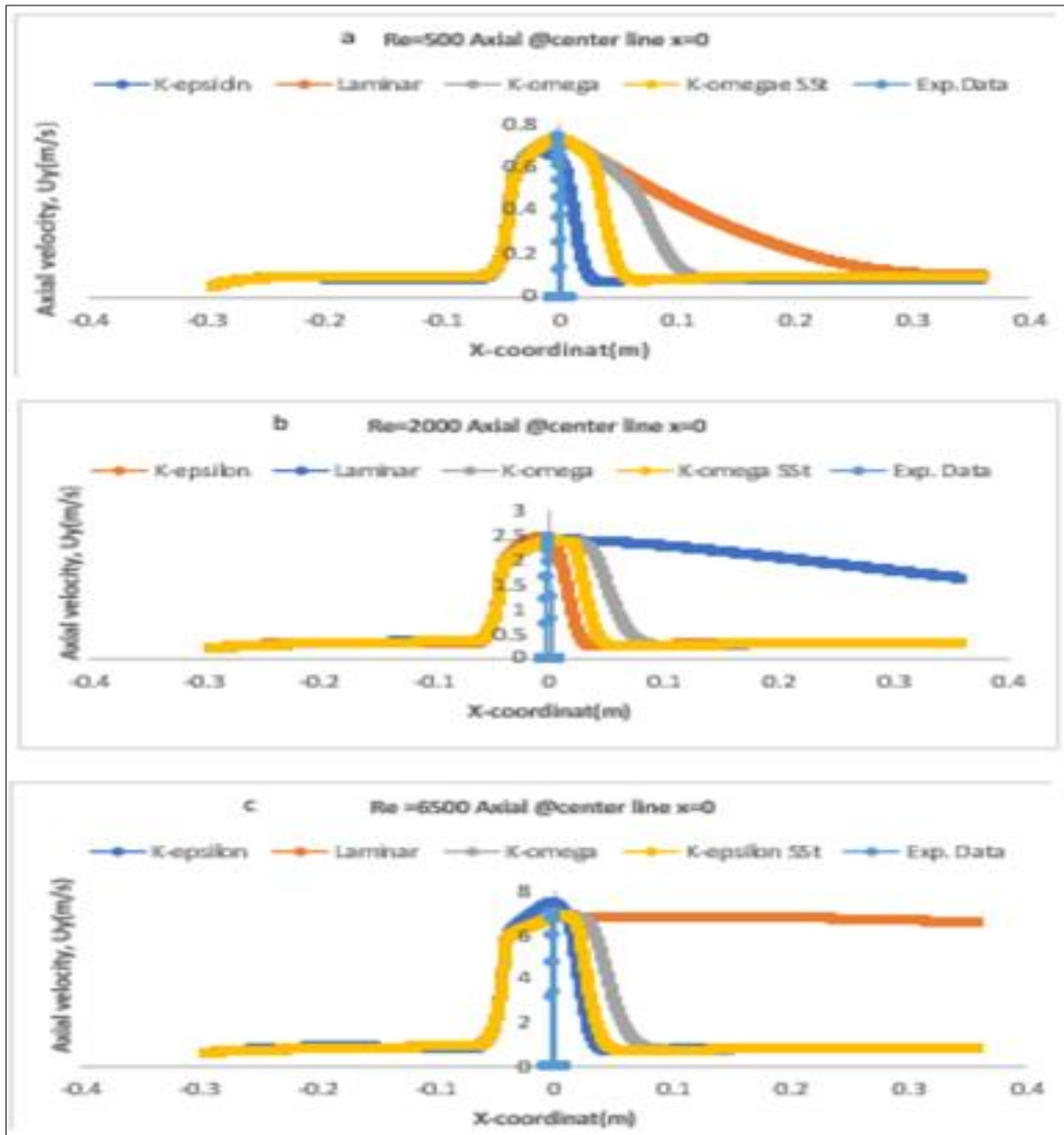


**Figure 16** Axial velocity at centreline  $Re_{th}$ . Of, a = 500, b = 2000 and c = 6500 at line  $X=0$

Figure 16 shows axial velocity centre line plots  $x = 0$  of four CFD models of K-epsilon, laminar, K-omega and k-omega SST and experimental data of 95% confident interval of [8]. From tube throat Reynolds number  $Re_{th} = 500$  Figure 16a, at inlet  $Re = 167$ . Table 5, shows experimental data solely laminar as  $Re = 500$  at throat. This matches experimental data, followed by K-omega and then K-omega SST. The K-epsilon SST is seen inward as the least match. This shows that Laminar is better models achieved at lower  $Re$ . At  $Re_{th} = 2000$  at inlet  $Re = 667$ , Table 5, Figure 16b, the K-omega model best matched experimental data, followed by K-omega SST and then K-epsilon SST. The laminar Model broke out experimental data half way, showing near transition flow of laminar to turbulence region. Also, Figure 16c, of  $Re_{th} = 6500$  at inlet  $Re = 2167$ , k-epsilon model best matched experimental data, followed by K-omega SST and K-omega. This inferred that K-epsilon model is better.

realized at higher  $Re$ . number turbulence model than K-omega SST and K-omega. However, laminar model performed poorly as it broke out entirely out of experimental data matched.

Wall pressure validation with experimental data for throat Reynolds number  $Re_{th} = 500, 2000$  and  $6500, X = 0$  in Figure 17

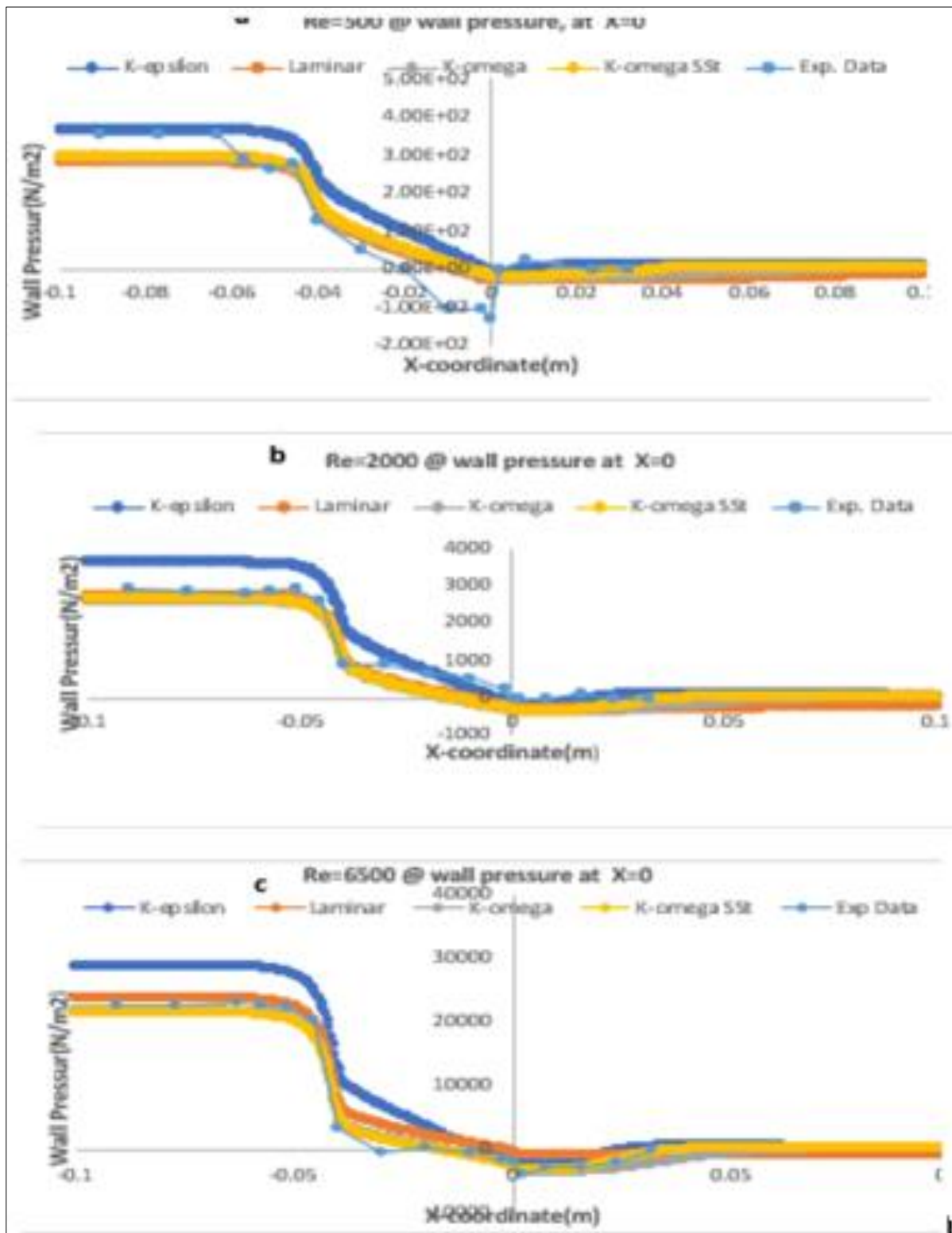


**Figure 17** Wall pressure validation at  $Re_t = 500, 2000$  and  $6500$   $X = 0$

The pressure variations were plotted in Figure 17a, b and c,  $x = 0$ , location of expansion. Procedure were done for  $Re_{th}$  at 500, 2000 and 6500, using K-epsilon, laminar, K-omega and K-omega SST models. Most models concided with experimental data, but was seen to drop lower at  $Re_{th} = 500$ , with small significant change at  $Re_{th} = 2000$  and matched well with  $Re_{th} = 6500$ . This show negligible centerline axial pressure gradient. Nevertheless, Figure 17a showed drop

in normalization point from 0 to  $-120\text{N/m}^2$  with experimental data counterbalanced at  $Re_{th} = 500$ . This problem could be from pressure difference in some experiments data run.

The k-epsilon flow has the biggest discrepancy (19.0%) between CFD simulations and experimental, at sudden expansion, wall pressure is negative. The biggest dichotomy in the measurements of wall pressure is at inlet. Table 8 shows margin of error between CFD simulations and experimental measurements. The turbulent flow agrees with CFD results, except for one data point which is anomalous.

**Table 8** Percentage of error for Wall Pressure at Inlet (-0.009 m)

Flow conditions	Maximum Difference at -0.09 m
Laminar Flow ( $Re = 500$ )	19.0%
Transitional Flow ( $Re = 2000$ )	17.2%
Turbulent Flow ( $Re = 6500$ )	8.10%

#### 4. Conclusion

A 2D-axisymmetric axial nozzle model geometry of faces 0.006 m, edges of inlet length of 0.23 m, out length of 0.36 m, throat 0.04 m, and slant length of 0.02304 m and axis of 0.653 is created in solid work and imported into ANSYS work bench 2020R1. Four simulation models of laminar, k-omega, k-omega SST and k-epsilon based on inlet throat  $Re_{th} = 500$ ,  $Re_{th} = 2000$  and  $Re_{th} = 6500$  were employed. The K-omega SST used for mesh independence determination for 0.0008, 0.0004 and 0.0002 element sizes.

Axial velocity at centreline for  $Re_{th} = 500$ ,  $Re_{th} = 2000$  and  $Re_{th} = 6500$  at line  $X = 0$ , showed that laminar model better at low Reynolds number, followed by transition of  $Re_{th} = 2000$ , then K-epsilon SST. At  $Re_{th} = 6500$  and inlet  $Re = 2167$ , k-epsilon model best matched experimental data.

Axial velocity at centreline for  $Re_{th} = 500$ , 2000 and 6500 at line  $X = 0$ . The results showed maximum difference of 77.4% for velocity at centerline at 0.08m and 19% for the wall pressure at -0.09m expansion at laminar region of  $Re = 500$ . Besides, 65.6% and 17.2% were obtained at transition of  $Re = 2000$ , agrees with CFD simulations. Nevertheless, at turbulent region  $Re = 6500$ , all models were in good agreement with 49.6% velocity centerline and 8.10% pressure drop, except in laminar legion.

#### Compliance with ethical standards

##### *Author contribution*

All authors contributed equally to this work.

##### *Funding*

This research received no specific grant from any funding agency in public, commercial, or not-for-profit sectors.

##### *Data availability statement*

The data that supports the findings of this study are available on request from corresponding author

##### *Disclosure of conflict of interest*

The authors declare that there is no conflicts of interest.

#### References

- [1] Bernsdorf J, Harrison SE, Smith SM, Lawford PV, Hose DR. Applying the Lattice Boltzman Technique to Biofluids: A Novel Approach to Simulate Blood Coagulation. *Computation Mathematics Application*. 2008; 1408 - 1414.

- [2] Burgreen GW, Antaki ZJ, Wu AJ. Holmes: Computational Fluid Dynamics as a Development Tool for Rotary Blood Pump. *Artificial Organs*. 2001; 336 - 340.
- [3] Fraser KH, Taskin ME, Zhang T, Griffith BP, Wu ZJ. A quantitative Comparison of Mechanical Blood Damage Parameters in Rotary Ventricular Assist Device: Shear Stress, Exposure time and Hemolysis Index. *Journal of Biomedical Engineering*. 2012, 3(1) 230- 240.
- [4] Huang IC. CFD Validations with FDA Benchmarks of Medical Devices Flows. 15th International LS-DYNA Users Conference. Detroit. 2018; 75 -95
- [5] ISO 14708 - 5. Implant for Surgery - Active Implantable Medical Devices Part 5. arlington, VA, USA. 2010.
- [6] ISO 5840 - 2. Cardiovascular Implant - Cardiac Valve Protheses part 2. VA, USA. 2015.
- [7] ISO 5840 - 3. Cardiovascular Implant - Cardiac Valve Protheses part 3. VA, USA. 2013.
- [8] Jain KL. Transition to Turbulence in an Oscillatory Flow Through Stenosis. *Biomechanics and Modeling in Mechanobiology Proceedings*. 2020; 8(4), 113 - 131.
- [9] Jain K, Ringstad G, Fide PK, Mardal KA. Direct Numerical Simulation of Transitional Hydrodynamics of the cerebrospinal Fluid in Chiari Malformation: The Role of Cranio-Vertebral Junction. *International Journal of Numerical Methods and Biomedical Engineering*. 2017; 7(3), 331 -342
- [10] Marsden AL, Bazilevs Y, Long CC, Behr M. Recent Advances in Computational Methodology for Simulation of Mechanical Circulatory Assist Devices. *Wiley Interdiscipline Review System Biomedics*. 2014; 4(1), 169 -188.
- [11] Raben JS, Hariharan P, Robinson R, Malinauskas R, Vlachos PP. Time-Resolved Particle Image Velocimetry Measurement with Wall Shear Stress and Uncertainty Quantification for the FDA Nozzle Model. *Cardiovascular Engineering Technology*. 2016; 6(2), 7 - 22.
- [12] Stewart SC, Eric G, Paterson Greg W, Burgreen P, Hariharan P, Matthew. Assesment of CFD Performance in Simulation of an Idealized Medical Device. *Results of FDA'S First Computational Inter-laboratory Study*. 2012, 37 -49
- [13] Sun C, Munn LL. Lattice -Boltzmann Simulation of Blood Flow in Digitized Vessel Networks. *Computation of Mathematics Application*. 2008; 5(3), 1594 - 1600.
- [14] White AT, Chong CK. Rotational Invariance in the Three Dimensional Lattice Boltzmann Method is Dependent on the Choice of Lattice. *International Journal of Computational Physics*. 2011; 3(1), 6367 -6378.
- [15] Zhang J, Johnson PC, Popel AS. Red Blood Cell Aggregation and Dissociation in Shear Flows Simulated by Lattice Boltzmann Method. *International Journal of Biomedicals*. 2008; 4(2), 47 -55.